Research Article

Umar Daraz, Tariq Mahmood Ansari*, Shafique Ahmad Arain, Muhammad Adil Mansoor, and Muhammad Mazhar

Effect of substrate temperature on structural, optical, and photoelectrochemical properties of Tl_2S thin films fabricated using AACVD technique

https://doi.org/10.1515/mgmc-2022-0017
received September 11, 2021; accepted June 29, 2022

Abstract: Thin films of thallium sulphide (Tl_2S) were grown on the FTO surface at three different temperatures (500°C, 550°C, and 600°C) using the aerosol-assisted chemical vapor deposition approach. A thallium diethyldithiocarbamate ($Tl[CNS_2(C_2H_5)_3]$) complex was used as a single-source precursor in tetrahydrofuran (THF) solvent under an inert atmosphere of argon in all deposition experiments. The impact of deposition temperature on structural, morphological, and optical properties of Tl_2S thin films was explored using different experimental techniques such as X-ray diffraction (XRD), field-emission scanning electron (FESEM) microscopy, and UV-visible spectrophotometry. XRD analysis specifies that crystallite size varies from 120 to 90 nm with the increase in temperature from 500°C to 600°C. FESEM results revealed that Tl_2S films were grown as hexagonal, petals, and marigold flower-like particles at 500°C, 550°C, and 600°C, respectively. UV-visible spectrophotometric analysis shows a decrease in band gap energies with temperature: 1.92 eV at 500°C, 1.72 eV at 550°C, and 1.42 eV at 600°C. The photoelectrochemical measurement in terms of linear sweep voltammetry confirms that the temperature variation has a significant effect on the photoconversion efficiency of Tl_2S thin films, and photocurrent density increases from 0.56 to 0.76 $mA{\cdot}cm^{-2}$ when the temperature is increased from 500°C to 600°C.

Keywords: metal chalcogenides, thallium sulfide, AACVD, bandgap, photocatalysts, LSV

1 Introduction

During the last few years, a lot of attention has been given to group 13 metal chalcogenides (Franz and Inoue, 2016; Guschlbauer et al., 2019). The main reason for this growing interest is their semiconductor nature, intrinsic vacancy structure, and the prospect of engineering in diverse stoichiometry (Jacobs-Gedrim et al., 2014; Kurosaki and Yamanaka, 2013; Ramanujam and Singh, 2017). Specifically, thallium chalcogenides have been constructed in numerous compositions due to the existence of thallium in stable oxidation states of +1 and +3. In particular, thallium–sulphur interactions in thallium sulphides are reported as Tl_2S, TlS, Tl_4S_3, and Tl_2S_5. Out of these polymorphs, only Tl_2S exists in a single oxidation state Tl(I), while TlS and Tl_4S_3 are mixed sulphides and represented as $Tl^+ [Tl^{3+} (S^{2-})_2]$ and $[Tl^+]_3[Tl^{3+} (S^{2-})_3]$, respectively (Chia et al., 2016; Elshaikh et al., 2004; Gamal et al., 2005; McGuire et al., 2005). Tl_2S is a black colour crystalline solid, found as the rare mineral carlinite, and has distorted anti-$CdCl_2$-like structure (Ashraf et al., 2004; Eda et al., 2011; Song et al., 2017).

Although thallium sulphides have been explored as optical, photoconductors, and photovoltaic materials but still have limited uses because of their toxicity (Estrella et al., 2002; Gomathi et al., 2015; Janickis and Stokiene, 2010; Marcano et al., 2012; Ramalingam et al., 2016). Another problem that comes up in the synthesis of nanothallium compounds is the formation of soluble metal hydroxide or oxy-hydroxides (Bhattacharya et al., 2002; Goudarzi et al., 2015; Lyons and Morris, 2002; Nejati et al., 2015). Therefore, few reports are available

* **Corresponding author: Tariq Mahmood Ansari,** Institute of Chemical Sciences, Bahauddin Zakariya University, Multan 60800, Pakistan, e-mail: tariqansari@bzu.edu.pk
Umar Daraz: Institute of Chemical Sciences, Bahauddin Zakariya University, Multan 60800, Pakistan
Shafique Ahmad Arain: Institute of Chemistry, Shah Abdul Latif University Khairpur, Sindh, Pakistan
Muhammad Adil Mansoor, Muhammad Mazhar: Department of Chemistry, School of Natural Sciences (SNS), National University of Sciences and Technology, H-12, Islamabad, Pakistan

on sulphides of thallium as compared to that of other members (Ga and In) of the same family. However, due to cost-effective benefit, thallium is still preferred over indium. Previously, the chemical bath deposition method was employed to deposit thallium sulphides thin films on various substrates (Estrella et al., 2001; Estrella et al., 2002). However, certain shortcomings such as wastage of solution after every experiment, requirement of exclusive catalysts, and formation of polycrystalline layers instead of targeted materials render this approach less attractive (Janickis and Stokiene, 2010).

Recently, (AACVD) has emerged as an efficient, cost-effective, and scalable technique to develop thin layers of materials with the desired composition on various substrates (Daraz et al., 2019, 2020, 2021). Unlike conventional chemical vapor deposition (CVD) techniques, AACVD only requires the solubility of the precursor, widening the options of different compounds to be used as single- and dual-source precursors (Ketchemen et al., 2018; Malik et al., 2010). Particularly, in AACVD, surface morphology and crystallite size of the end product can exclusively be controlled by tuning the deposition parameters such as deposition temperature, deposition time, and nature of solvents (Ehsan et al., 2012; Jafer et al., 2021). Therefore, AACVD can be used to fabricate a variety of metal chalcogenide, metal carbide, and metal oxide nanoparticles and thin films of desired morphology employing different precursors such as dithiocarbamate, xanthates, dithiophosphinate, dithiophosphate, and dithiocarboxylate. For example, Khan et al. (2015, 2017) deposited lead sulphide and copper sulphide thin films on the glass substrate using xanthate precursors via the AACVD approach. In other works, Khan et al. (2018, 2019) reported a novel selenium complex, i.e., tris (selenobenzoato) antimony(III) and used as a single-source precursor for the synthesis of antimony sulphide (Sb_2Se_3) nanorods and thin films using the AACVD technique. Dithiocarbamates and xanthates are two often employed precursors in AACVD, with the former having the advantage of being able to grab and store metals in a different range of oxidation states. Furthermore, dithiocarbamates can accommodate a wide range of alkyl groups, resulting in a diverse set of precursors (Sarker and Hogarth, 2021). Here, we report the deposition of thallium sulphide (Tl_2S) thin films via the AACVD technique on the FTO substrate at three different deposition temperatures. All depositions were achieved under an inert atmosphere of argon gas utilizing THF solution of thallium diethyldithiocarbamate as a single-source precursor.

2 Results and discussion

Complex **1** was synthesized by the double displacement reaction of sodium diethylthiocarbamate with thallium nitrate in methanol solvent according to the following equation:

$$\mathrm{Tl(NO_3)_3 + 3NaS_2CN(C_2H_5)_2} \xrightarrow{\text{Methanol}} \mathrm{Tl[(S_2CN(C_2H_5)_2]_3 + 3NaNO_3} \quad (1)$$

The synthesized complex (**1**) was obtained in 82% yield and characterized by melting point, elemental analysis (CHNS), thermogravimetric analysis (TGA), ^{1}H NMR, ^{13}C NMR, and infrared (IR) spectroscopy. The IR spectra of complex **1** have been observed with strong absorption bands over regions 2,972 and 2,925 cm^{-1}. These bands confirm the presence of the C–N bond and C–H stretching of the alkyl group in the complex. The absorption peaks in the functional group region at 1,495 and 1,430 cm^{-1} confirm to C═S and C–S bonds in the complex. The values at 1,265–782 cm^{-1} are indications of the metallic complexes of the marcapto group with thiosemicarbazones. A band in the former at 840–782 cm^{-1} is attributed to (C═S). It may be concluded that there is a contribution from (C═S) in both regions, but absorption in the lower region represents the more nearly pure C═S stretching vibration. Examination of the spectra of *N*-ethyl substituted thiosemicarbazones indicates that, even in this 840–805 cm^{-1} region, C═S stretching is coupled with other vibrations, perhaps S–C–N stretching (Figure A1). In the ^{1}H NMR spectrum, a triplet appeared at 1.327 ppm due to sp^3-hybridized C–H along with the absorbance of 18 protons in the aliphatic region confirming the formation of the targeted complex. A quartet of 12 protons appeared at 3.804 ppm, which confirms the neighboring protons. These aliphatic protons have been assigned according to their chemical shift with multiplicity and coupling constant (Figure A2). The ^{13}C NMR spectrum also confirms the aliphatic carbons with saturated and unsaturated behaviour in respective chemical shifts. Absorption bands at 42.07, 52.11, and 156.20 ppm confirm the presence of aliphatic at the ^{13}C position and quaternary carbon in the metallic complex. Spectrum confirms the aliphatic carbons of the ethyl group with primary and secondary carbons. The quaternary carbon attached to N and S atoms is also indicated by a high chemical shift in the targeted complex (Figure A3). TGA shows that complex **1** decomposes in a single step and gives a stable end product after 300°C (Figure A4). Moreover, complex **1** is easily soluble in common organic

solvents such as THF, toluene, and chloroform which ensures its ability to use as SSP in the AACVD process.

2.1 XRD analysis

Fabricated Tl_2S thin films were analysed by XRD to examine phase purity and degree of crystallinity. The attained peak patterns in all three cases (Figure 1) matched well with ICOD card no. [96-901-2278], having space group of *R*3 and cell parameters of $a = b = 12.150$, $c = 18.190$ Å. Those peaks, which are labelled by (●) at 2θ positions of 20.79, 25.40, 29.56, 33.22, 39.33, 44.49, 49.88, 52.42, and 54.66° relate lattice planes of (104), (300), (303), (125), (036), (009), (505), (309), and (229) respectively, specified the growth of hexagonal crystalline (carlinite) Tl_2S in all of the fabricated films. The remaining low intensity peaks designated by (▼) at 2θ values of 63.22°, 67.39°, and 79.02° agreed to the SnO_2 layer of the FTO substrate. Further, all XRD have shown a 29.56° peak, which designates that the carlinite particles are positioned in the (303) direction. A sticky matching pattern is available in Figure A5. The inclusive XRD patterns remain unaffected by the rise in deposition temperature except an obvious surge in the peak strengths, which demonstrates that crystallinity improves with temperature.

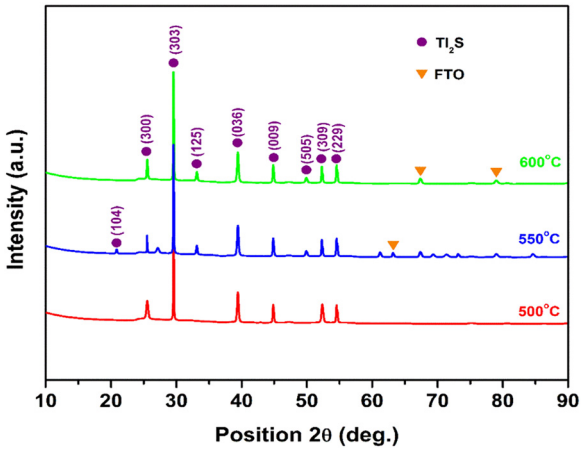

Figure 1: X-ray diffraction (XRD) patterns of Tl_2S thin films deposited on the FTO substrate at three different temperatures using the AACVD approach.

2.2 Surface morphology

Figure 2a–c shows the surface morphologies of Tl_2S thin films, explored using FESEM analysis. At relatively low temperature (500°C), films are grown as asymmetrical hexagonal particles having well-defined sharp boundaries.

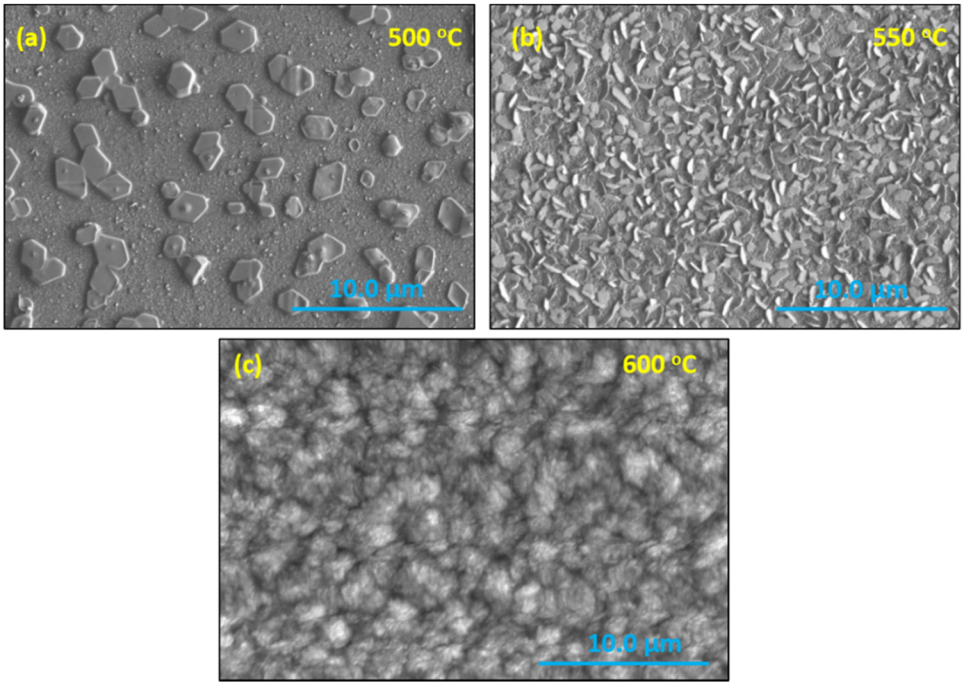

Figure 2: FESEM micrographs of Tl_2S thin films deposited on FTO substrate via AACVD technique at three different temperatures: (a) 500°C, (b) 550°C, and (c) 600°C.

At 550°C, these hexagonal particles began to deteriorate and change into petal-like shapes that are finely separated and still possess visible boundaries. When the temperature is further increased to 600°C, a thin layer of Tl_2S particles takes the shape of a marigold flower, thus presenting a porous texture and occupying the entire surface of the FTO substrate. It is well recognized that the morphology of any material has prime importance in governing its efficacy in photoelectrochemical (PEC) applications. Apparently, the hexagonal geometry of Tl_2S obtained at 500°C has a uniform texture, but particles are widely distributed. These wide distributions reduce the light-harvesting capability of materials as photogenerated charge carriers will recombine as soon as they are formed and fail to develop strong interaction with substrate surfaces. Whereas petals obtained at 550°C are comparatively closely packed and believed to capture a substantial part of solar energy to respond better as a photoelectrode in PEC studies. However, a close look at Figure 2b divulges that there are still some gaps present between particles and the FTO surface is visible. Therefore, Tl_2S thin films were deposited at a further higher temperature of 600°C resulting in a marigold flower-like growth that completely covers the FTO surface and is thought to have improved photocatalytic response. When stimulated by solar radiation, this marigold flower-like arrangement presents a better surface area to interact with electrolytes, help the movement of photogenerated electrons throughout the material, and consequently, better photocatalytic activity is achieved.

In AACVD, thin film deposition may follow a homogeneous or/and heterogeneous mechanism depending on the temperature of the reacting zone. At relatively low temperature (500°C), the heterogenous route is dominated, and precursor aerosols may interact and get adsorbed onto the substrate surface, followed by evaporation, vaporization, precipitation, and decomposition. Consequently, high-quality thin films with excellent purity and adhesive strength are designed (Figure 2a). By increasing the temperature to 550°C, the solvent evaporated while the precursor vapourized before the adsorption phenomenon as aerosols absorb more heat during their passage to the delivery tube resulting in the homogenous route to thin film development (Figure 2b). Moreover, at a further high temperature of 600°C, all processes such as solvent decomposition and aerosol vaporization along with precipitation and thermolysis complete in a single step. As a result, very small-sized particles reach the substrate surface and aggregate of which gives nanoscaled thin films of porous texture by homogenous mechanism. This nanoscaled distribution covered the entire surface but had weak adhesion to the substrate and presented a base for the additional development of a porous layer of asymmetrical structure (Figure 2c). In this particular case, all depositions were performed in THF solvent that offered pale yellow colour Tl_2S thin films of excellent adhesion strength to the FTO substrate at 500°C and 550°C. Whereas the films fabricated at 600°C displayed dark yellow colour and less adhesion strength to the FTO substrate and failed the scotch tape test.

2.3 EDX and XPS studies

EDX analysis confirms the presence of Tl and S in Tl_2S thin films (Figure A6) but exact quantification is repressed by the overlapping of characteristics X-ray signals of both the components (Tl and S) at about 2.3 keV. Therefore, an XPS study was carried out to investigate the elemental composition and oxidation states of individual elements, and the results are shown in Figure 3. The XPS survey scan of Tl_2S thin films fabricated at 600°C identified the distinct signals at binding energies of 15.15, 118.46, 122.89, 382.76, 405.59, and 610.44 for Tl and 161.5 and 167.5 eV for S (Figure 3a). This verifies the presence of Tl and S as major surface components in an atomic ratio of 2:1, respectively. The high-resolution narrow scan of Tl 4 f furnished spin-orbital splitting at binding energies of 118.4 and 122.9 eV (Tl $4f_{7/2}$ and Tl $4f_{5/2}$), which correlates tothe +1 oxidation state of Tl (Figure 3b). Similarly, a narrow scan of S 2p presented a doublet state at 161.5 and 167.5 eV, relating to the presence of sulphur (S) in the sulphide state (Figure 3c). These XPS findings support EDX and XRD results and approve the formation of pure phase Tl_2S (carlinite).

2.4 FTIR and Raman spectroscopy

To further ensure phase purity, the Tl_2S films fabricated at 600°C were subjected to FTIR analysis, and the results are illustrated in Figure 4. There is no obvious peak present in the wavelength region of 1,000–1,500 cm^{-1} that confirms the absence of organic impurity. The FTIR fingerprint region showed a strong peak at 595 cm^{-1} due to Tl-S stretching and a weak starching mode at 630 cm^{-1} corresponding to the FTO substrate. In contrast, Raman spectroscopic analysis (inset of Figure 4) provided phone modes at 89.5, 140, 160.7, 177, 197, and 282.2 cm^{-1}. Two

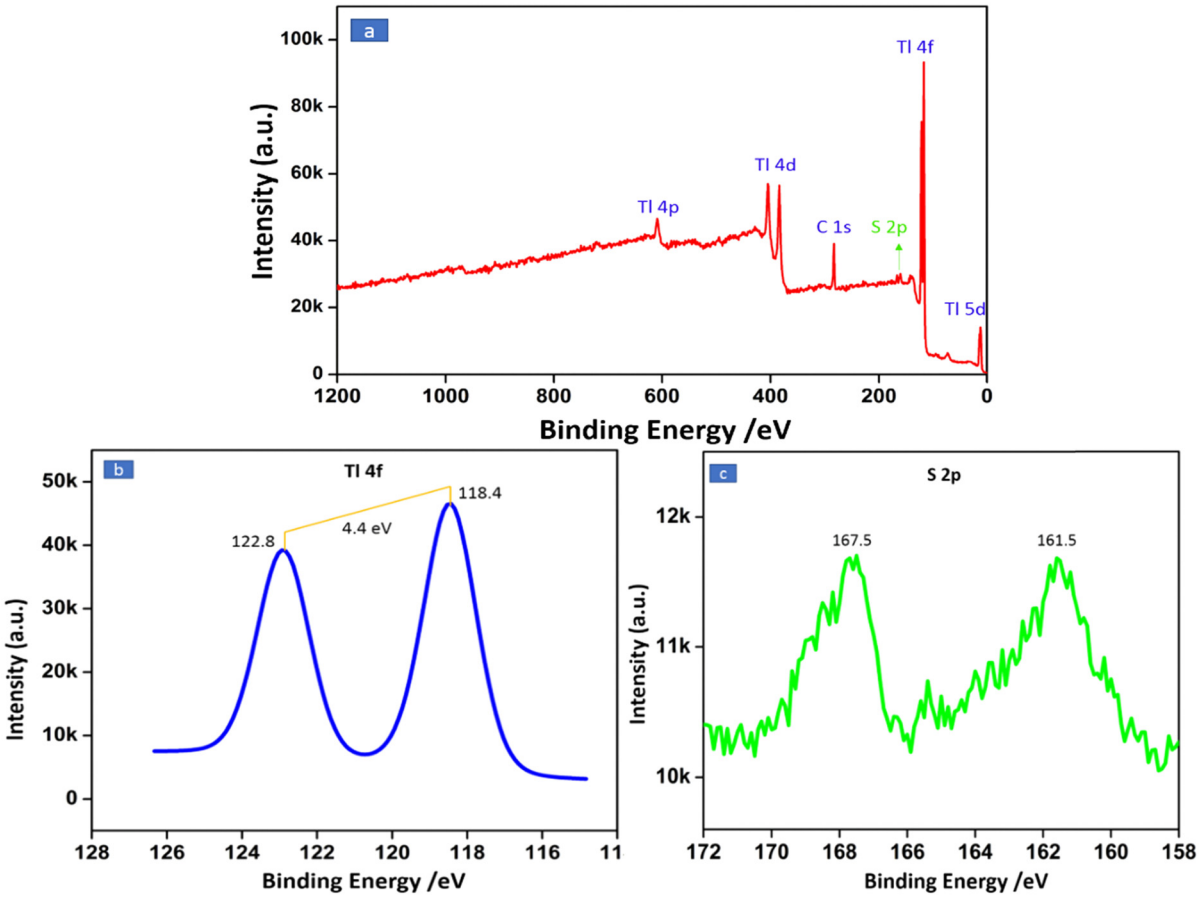

Figure 3: XPS results of Tl_2S thin films fabricated at 600°C using THF solution of complex **1** via AACVD approach: (a) survey scan, (b) Tl 4f, and (c) S 2p.

sharp peaks at 160 and 282.2 cm^{-1} were assigned to E_u and A_{2u} vibration modes. The first mode is degenerate, that is why additional vibrational modes are observed, which can be attributed to the defects in the crystal structure. The sharp and highly intense peaks in Raman spectra of Tl_2S thin films fabricated at 600°C depicts well crystalline nature of material that exhibits greater polarization. These FTIR and Raman findings are in good agreement with reported data and confirm that sulphur is sandwiched between two thallium atoms (Tl–S–Tl) in Tl_2S films. Moreover, both the FTIR and Raman analysis elucidated the pure nature of Tl_2S films as no potential impurity peaks due to oxygen is observed.

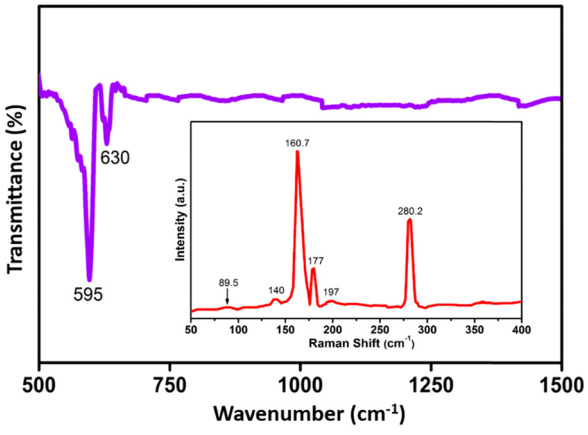

Figure 4: FTIR and Raman (inset) spectra of Tl_2S thin films fabricated at 600°C on the FTO substrate using the AACVD technique.

2.5 Optical studies

Light-absorbing capability and band gaps of fabricated films were investigated using UV-visible (UV-Vis) spectrophotometry, and the results are depicted in Figure 5. UV-Vis absorption spectra were recorded in the wavelength range of 350–900 nm, which shows that the optical absorbance of all of the Tl_2S films increases linearly towards lower wavelength and gives λ_{max} at 308 nm

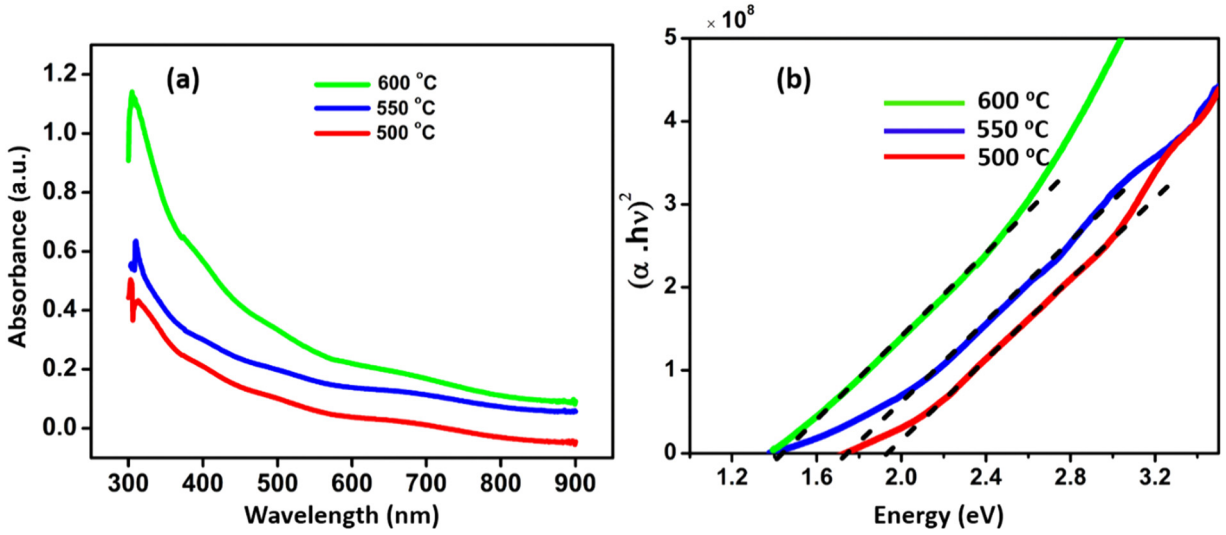

Figure 5: (a) UV-Vis absorption spectra and (b) optical band gaps of Tl_2S thin films fabricated at three different temperatures on the FTO substrate.

(Figure 5a). These results confirm the active optical nature of the deposited films as these absorb light in the whole UV and visible region of the solar spectrum. Moreover, the optical absorbance of the films developed at 600°C improved significantly in the visible section (red shift), which is associated with the uniform texture and better surface morphology which results in less scattering and good absorption than that of the films deposited at 500°C and 550°C. The band gap values are estimated by using Tauc's equation, and it comes out 1.92, 1.72, and 1.42 eV for the Tl_2S thin films fabricated at three different substrate temperatures 500°C, 550°C, and 600°C, respectively (Figure 5b). The films deposited at high temperature exhibit low band gap energy that corresponds to effective generation and separation of charge carriers. This might be attributed to the small crystallite size as well.

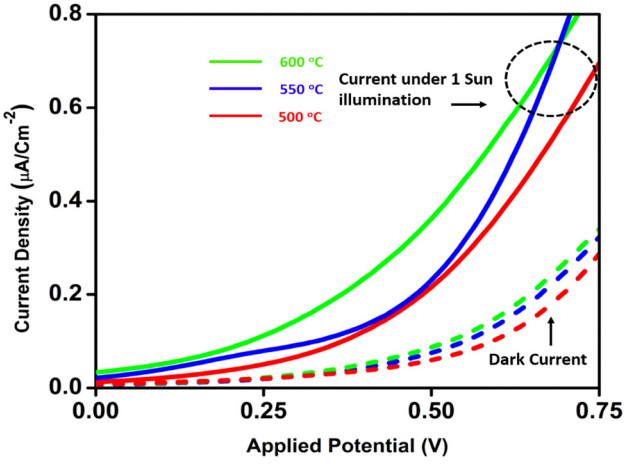

Figure 6: LSV outcomes of Tl_2S thin films deposited on the FTO substrate using three different temperatures via the AACVD technique.

2.6 Photoelectrochemical studies

The photoactivity of fabricated Tl_2S thin films and the role of substrate temperature were studied by using linear sweep voltammetry (LSV) technique. The study was carried out in conventional three electrodes electrochemical cells by employing synthesized material as an anode, platinum wire as a counter electrode, and Ag/AgCl in 3 M as a reference electrode in 0.1 M Na_2S aqueous solution as an electrolyte. Figure 6 shows that all of the Tl_2S films offered negligible current in the dark, but considerable photocurrent is achieved when irradiated by a 1 Sun solar simulator. The Tl_2S thin films developed at 500°C delivered 0.56 mA·cm^{-2}, while that developed at 550–600°C provided 0.76 mA·cm^{-2} photocurrent density at 0.7 V. These results prove that substrate temperature has a significant effect on the photoconductive nature of Tl_2S thin films and it can be correlated to the particle size and their distribution on the substrate as explained in XRD and FESEM analysis. Small crystallite size and uniform distribution of the end product in films fabricated at higher temperatures efficiently reduce the time and energy for the promotion of an electron from the valence band to the conduction band. As a result, a hole is generated in the valence band that oxidizes the water molecule to produce

oxygen, and promoted electron is picked up by hydroxy ion to generate hydrogen. It is also evident from the voltammogram that the applied potential also plays a very important role in the creation of photogenerated charge carriers as the photocurrent density of the thin films prepared at 550°C increases steadily from 0.00 to 0.34 V and then suddenly increases from 0.35 to 0.7 V. The same behaviour is not observed in thin films made at 500–600°C, and their photocurrent increases steadily with voltage.

3 Conclusion

Thallium sulphide (Tl_2S) thin films have been successfully deposited on the FTO substrate at three different temperatures ranging from 500°C to 600°C, using THF solution of the $Tl[CNS_2(C_2H_5)_3]$ complex via the AACVD technique. Structural, morphological, and optical features of fabricated films were revealed using XRD, FESEM, and UV-Vis spectrophotometry techniques, respectively. The results demonstrate that crystallite size, surface texture, and band gap can easily be tuned by varying the temperature in the AACVD technique. Moreover, PEC applications in terms of LSV confirm the photoactive nature of these Tl_2S films and suggest that by increasing temperature, photocurrent density is significantly enhanced. So, in light of these results, it may be concluded that Tl_2S thin films are a very good candidate for solar cells and PEC devices and for producing hydrogen from water by a process known as solar-driven photocatalytic water splitting.

Experimental section

As thallium is a highly toxic material, recommended precautions for the handling and disposal of thallium wastes are followed (Appendix).

Synthesis of $Tl[CNS_2(C_2H_5)_3]$ (1)

The purified crystals of sodium diethyl dithiocarbamate (0.50 g, 3 mmol) were dissolved in 20 mL of methanol solvent and transferred to a 100 mL three-necked round bottom flask which was connected to a dropping funnel, a reflux condenser, and an inert gas line. After that, 0.444 g (1 mmol) of thallium nitrate ($Tl(NO_3)_2{\cdot}5H_2O$) was added, which turned the colour of solution orange yellow, and was stirred continuously for 30 min. Filtration and slow evaporation of the reaction mixture afforded orange-yellow coloured crystals of precursor **1**, tris-(*N*,*N*′-diethyldithiocarbamato) thallium(III) complex. Yield (82%), m.p. 180°C. The CHNS measurements attained C, 27.03%; H, 4.30%; N, 5.35%; S, 28.37%; $TlC_{15}N_3S_6H_{30}$ requires C, 27.76%; H, 4.62%; N, 6.47%; S, 29.58%. IR (υ_{max}/cm^{-1}) 2,972m, 2,925w, 1,495s, 1,430s, 1,350m, 1,265s, 1,205s, 1,144s, 1,073m, 978s, 908s, 840s, 782m, 607w, 570s, 498w. ^{1}H NMR δ_H (400 MHz, $CDCl_3$): 1.327–1.568 ppm [18H, s, 6(–CH_3)] and 3.769–3.820 ppm [12H, m, 3(–CH_2)]; ^{13}C NMR δ_H (400 MHz, $CDCl_3$): 11.370–13.660 ppm [w, 6(–CH_3)], 49.995–52.211 ppm [w, 6(–CH_2)], and 192.92 ppm [m, 1(C–N)].

Deposition of Tl_2S thin films by AACVD

Deposition of Tl_2S thin films on the fluorine-doped tin oxide (FTO) surface was achieved at three different temperatures of 500°C, 550°C, and 600°C by AACVD technique using THF solution of $Tl[CNS_2(C_2H_5)_3]$ complex as a single-source precursor. A typical procedure involves the cutting of FTO substrates into suitable dimensions of 2 cm × 1 cm ($L \times W$) followed by ultrasonic washing with deionized water and acetone and then stowed in ethanol. After sometimes, these FTO substrates were kept horizontally within the reactor tube which is then placed inside a tube furnace. After achieving the desired deposition temperatures, 10 mL of the precursor solution was taken in a 250 mL round bottom flask and placed at an ultrasonic humidifier. The ultrasonic humidifier transformed the precursor solution into aerosols which were transported into the deposition (reaction) zone by the argon gas, where the deposition was carried out for 40 min. The volatile components and by products were ventilated by the exhaust system of the fuminghood. Finally, the ultrasonic humidifier and tube furnace were shut down, and argon gas was allowed to flow for some time (15 min) to ensure thorough deposition. These deposition experiments were performed repetitively in order to confirm the reproducibility of the end product.

Thin films characterization

The structural, morphological, and optical characterization of fabricated Tl_2S thin films was achieved using non-

destructive experimental techniques such as XRD, FTIR, Raman spectroscopy, EDX, XPS, FESEM, and UV-Vis spectrophotometry, respectively. The XRD analysis was carried out using the PAN analytical, X'Pert High Score diffractometer working at an accelerating voltage of 40 kV and 40 mA current. The XPS analysis was performed on ULVAC-PHI, Quantera II, having X-ray monochromatic radiation of Al-Kα (1486.8 eV), and a reference beam of C 1s (284.6 eV) was used to calibrate the binding energies. FESEM studies were completed by employing a field-emission scanning electron microscope (FESEM, FEI Quanta 400) coupled with an energy-dispersive X-ray (EDX) spectrometer (INCA Energy 200) operating at an accelerating voltage of 20 kV and a working distance of 9.2 mm.

Optical and PEC measurements

The optical measurements of all Tl_2S thin films were completed on an UV-Vis spectrophotometer (The Lambda 35 Perkin-Elmer) in the spectral region of 380–900 nm by utilizing a bare FTO substrate as a reference to minimize the substrate effect in the spectrum. The surface thickness of Tl_2S thin films on the FTO surface was determined on the KLA Tencore P-6 surface profilometer, and it comes out 380, 400, and 430 nm at 500°C, 550°C, and 600°C, respectively. The PEC potential of prepared Tl_2S thin films in terms of LSV was probed on a potentiostat (Eco Chemie micro-Autolab type III) connected with a conventional electrochemical workstation of three electrodes. All measurements were carried out in 0.01 M Na_2S aqueous solution (electrolyte) using Ag/AgCl/3 M KCl as a reference and platinum wire as a counter electrode, respectively. Fabricated Tl_2S thin films with an effective area of 1 cm^2 were used as working electrodes and were illuminated by a solar simulator AM 1.5 classes A (Solar Light 16S-300) of light intensity 100 $mW{\cdot}cm^{-2}$.

Acknowledgment: This research article is a part of PhD Thesis of Dr. Umar Daraz. The research was carried out under the generous grant of the Higher Education Commission (HEC), Islamabad, Pakistan. Umar Daraz is thankful to Dr. Tariq Riaz Bhutta for discussing NMR spectra. The authors are also grateful to the Institute of Chemical Sciences (ICS), Bahauddin Zakariya University (BZU), Multan, Pakistan, and the University of Malaya (UM), Kuala Lumpur, Malaysia for offering research facilities to accomplish this work.

Funding information: Authors state no funding involved.

Author contributions: Umar Daraz: experimental data collection, writing; Tariq Mahmood Ansari: project administration, supervision, writing; Shafique Ahmad Arain: guidance and writing; Muhammad Adil Mansoor: discussion and joint writing in photoelectrochemical studies; Muhammad Mazhar: project resources and guidance.

Conflict of interest: Authors state no conflict of interest.

References

Ashraf I., Elshaikh H., Badr A., Characteristics of photoconductivity in Tl_2S layered single crystals. Phys. Status Solidi., 2004, 241(4), 885–894.

Bhattacharya R., Xing Z., Wu J., Chen J., Yang S., Ren Z., et al., Superconducting thallium oxide and mercury oxide films. Physica C Supercond., 2002, 377(3), 327–332.

Chia X., Ambrosi A., Sofer Z.K., Luxa J., Sedmidubský D., Pumera M., Anti-MoS_2 nanostructures: Tl2S and its electrochemical and electronic properties. ACS Nano, 2016, 10(1), 112–123.

Daraz U., Ansari T.M., Arain S.A., Mansoor M.A., Mazhar M., Structural, topographical and optoelectronic properties of $ZnIn_2S_4$ thin films deposited from dual source using aerosol assisted chemical vapour deposition (AACVD) technique. J. Chem. Soc. Pak., 2020, 42(2), 155–163.

Daraz U., Ansari T.M., Arain S.A., Mansoor M.A., Mazhar M., Study of solvent effect on structural and photoconductive behavior of ternary chalcogenides $InBiS_3$-In_2S_3-Bi_2S_3 composite thin films deposited via AACVD. Main Group Met. Chem., 2019, 42(1), 102–112.

Daraz U., Ansari T.M., Arain S.A., Mansoor M.A., Mazhar M., Hussain F., Fabrication, characterization, and photocatalytic performance of ternary cadmium chalcogenides $CdIn_2S_4$ and $Cd_{7.23}Zn_{2.77}S_{10}$ - ZnS thin films. Main Group Met. Chem., 2021, 44(1), 39–50.

Eda G., Yamaguchi H., Voiry D., Fujita T., Chen M., Chhowalla M., Photoluminescence from chemically exfoliated MoS_2. Nano Lett., 2011, 11(12), 5111–5116.

Ehsan M.A., Ming H.N., Misran M., Arifin Z., Tiekink E.R., Safwan A.P., et al., Effect of AACVD Processing Parameters on the Growth of Greenockite (CdS) Thin Films using a Single-Source Cadmium Precursor. Chem. Vap. Depos., 2012, 18(7–9), 191–200.

Elshaikh H., Ashraf I., Badr A., Special Technique for Growing Tl_4S_3, Anisotropy of Electrical Conduction and Photophysical Properties. J. Phys. Chem. B, 2004, 108(31), 11327–11332.

Estrella V., Mejía R., Nair M., Nair P., Optical and electrical properties of thallium sulphide and $Tl_xM_yS_z$ (M = Cu, Bi, Sb) thin films. Mod. Phys. Lett. B, 2001, 15(17), 737–740.

Estrella V., Nair M., Nair P., Crystalline structure of chemically deposited thallium sulfide thin films. Thin Solid Films, 2002, 414(2), 281–287.

Franz D., Inoue S., Advances in the development of complexes that contain a group 13 element chalcogen multiple bond. Dalton Trans., 2016, 45(23), 9385–9397.

Gamal G., Abou Zied, M., Ebnalwaled A., Electronic properties of red p-type Tl_2S_5 single crystals. Chin. Phys. Lett., 2005, 22(6), 1530.

Gomathi G., Thirumaran S., Ciattini S., Anagostic, mono and hexa-hapta interactions in Tl (I) dithiocarbamates: A new precursor for the preparation of Tl_2S nanoparticles. Polyhedron, 2015, 102, 424–433.

Goudarzi M., Ghanbari D., Salavati-Niasari M., Photo-catalyst thallium sulfide: synthesis and optical characterization different morphologies of Tl_2S nanostructures. J. Mater. Sci.; Mater Electron, 2015, 26(11), 8798–8806.

Guschlbauer J., Vollgraff T., Sundermeyer J.R., Homoleptic Group 13 Trimethylsilylchalcogenolato Metalates [M ($ESiMe_3$) 4]−(M = Ga, In; E = S, Se): Metastable Precursors for Low-Temperature Syntheses of Chalcogenide-Based Materials. Inorg. Chem., 2019, 58(22), 15385–15392.

Jacobs-Gedrim R.B., Shanmugam M., Jain N., Durcan C.A., Murphy M.T., Murray T.M., et al., Extraordinary photoresponse in two-dimensional In_2Se nanosheets. ACS Nano, 2014, 8(1), 514–521.

Jafer R., Iqbal J., Shahid M., Wageh S., Growth of dimensionally favoured TiO_2 morphologies by AACVD and their recognized performance as LIB anode. Ceram. Int., 2021, 47(5), 6848–6853.

Janickis V., Stokiene R., Thallium sulfides and their layers on polyamide surface. Chemija, 2010, 21(1), 17–32.

Ketchemen K.I., Mlowe S., Nyamen L.D., Ndifon P.T., Revaprasadu N., O'Brien P., CdS thin films deposition by AACVD: effect of precursor type, decomposition temperature and solvent. J. Mater. Sci.: Mater. Electron, 2018, 29(17), 14462–14470.

Khan M.D., Hameed S., Haider N., Afzal A., Sportelli M.C., Cioffi N., et al., Deposition of morphology-tailored PbS thin films by surfactant- enhanced aerosol assisted chemical vapor deposition. Mater. Sci. in Semicond. Process., 2015, 46, 39–45.

Khan M.D., Malik M.A., Akhtar J., Mlowe S., Revaprasadu N., Phase pure deposition of flower-like thin films by aerosol assisted chemical vapour deposition and solvent mediated structural transformation in copper sulfide nanostructures. Thin Solid Films, 2017, 638, 338–344.

Khan M.D., Amir M., Sohail M., Sher M., Akhtar J., Malik M.A., et al., Novel single source precursor for synthesis of Sb2Se3 nanorods and deposition of thin films by AACVD: Photo-electrochemical study for water reduction catalysis. Sol. Enrergy, 2018, 169, 526–534.

Khan M.D., Malik M.A., Revaprasadu N., Progress in selenium based metal-organic precursors for main group and transition metal selenide thin films and nanomaterials, Coord. Chem. Rev., 2019, 388, 24–47.

Kurosaki K., Yamanaka S., Low-thermal-conductivity group 13 chalcogenides as high-efficiency thermoelectric materials. Phys. Status Solidi, 2013, 210(1), 82–88.

Lyons D.M., Morris M.A., Synthesis and characterization of a novel perovskite-like phase of thallium oxide. Cryst. Growth Des., 2002, 2(5), 427–430.

Malik M.A., Afzaal M., O'Brien P., Precursor chemistry for main group elements in semiconducting materials. Chem. Rev., 2010, 110(7), 4417–4446.

Marcano D., Gerasimchuk N., Nemykin V., Silchenko S., Synthesis, characterization, and studies of coordination-Polymeres with Isomeric Pyridylcyanoximes: Route to Metal Ribbons with very short Tl··· Tl Separations. Cryst. Growth Des., 2012, 12(6), 2877–2889.

McGuire M.A., Reynolds T.K., DiSalvo F.J., Exploring thallium compounds as thermoelectric materials: Seventeen new thallium chalcogenides. Chem. Mater., 2005, 17(11), 2875–2884.

Nejati M.L., Esmaeili B.K.A., Salavati N.M., Safardoust H., Synthesis and characterization of SnO_2 nanostructures prepared by a facile precipitation method. J. Nanostruct., 2015, 5(1), 47–53.

Ramalingam K., Rizzoli C., Sivagurunathan G.S., Mono and trivalent thallium–sulfur interactions and their influence on the formation of nano thallium sulphide: single crystal X-ray structural and spectral studies on thallium (i)/(iii)–cyclohexylpiperazine dithiocarbamates. New J. Chem., 2016, 40(3), 2489–2500.

Ramanujam J., Singh U.P., Copper indium gallium selenide based solar cells–a review. Energy Environ. Sci., 2017, 10(6), 1306–1319.

Sarker, J.S., Hogarth, G., Dithiocarbamate complexes as single sources precursors to nanoscale binary, ternary and quaternary metal sulphides, Chem. Rev., 2021, 121, 6057–6123.

Song N., Wang Y., Yu W., Zhang L., Yang Y., Jia, Y., Electronic, magnetic properties of transition metal doped Tl_2S: First-principles study. Appl. Surf. Sci., 2017, 425, 393–399.

Appendix

Recommended precautions for of handling toxic thallium materials

1. Thallium and its compounds are reported to be toxic; therefore, all experiments should be carried out under a controlled and enclosed environment of argon and use of local exhaust ventilation; otherwise, at high temperature toxic thallium oxides will be formed.
2. Clothing worn in areas of exposure to thallium dust or vapor should be restricted to the workplace and stored in special lockers. Wear impermeable gloves and protective work clothing as necessary.
3. In case of inhalation, eye contact, or touch, wash/eye skin immediately, remove to fresh air, keep warm and quiet, and give oxygen if breathing is difficult.
4. Symptoms of ingestion (intentional/unintentional) are abdominal pain and vomiting, extreme pain in the extremities, lethargy, and hair loss.
5. Dispose of in accordance with Federal, State, and Local regulations. Dilute thallium solutions may be buried in an approved dump or landfill where there is no risk of contamination of surface or groundwater. Local legislation regarding the disposal of toxic wastes must be complied with.

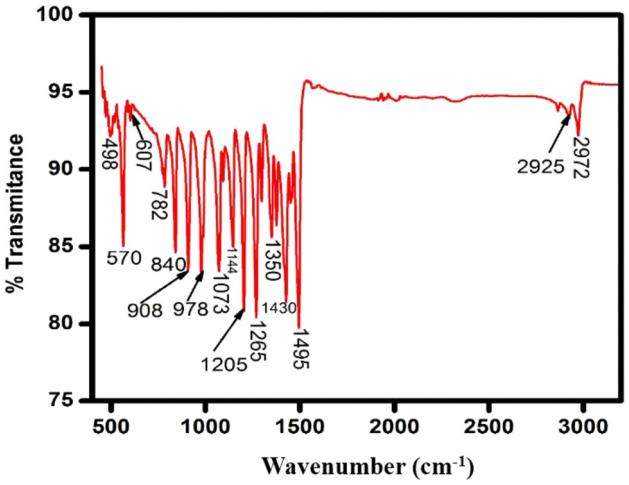

Figure A1: FTIR spectrum of complex **1** synthesized by the metathetical reaction of thallium nitrate trihydrate with sodium diethyl dithiocarbamate ligand in methanol solvent.

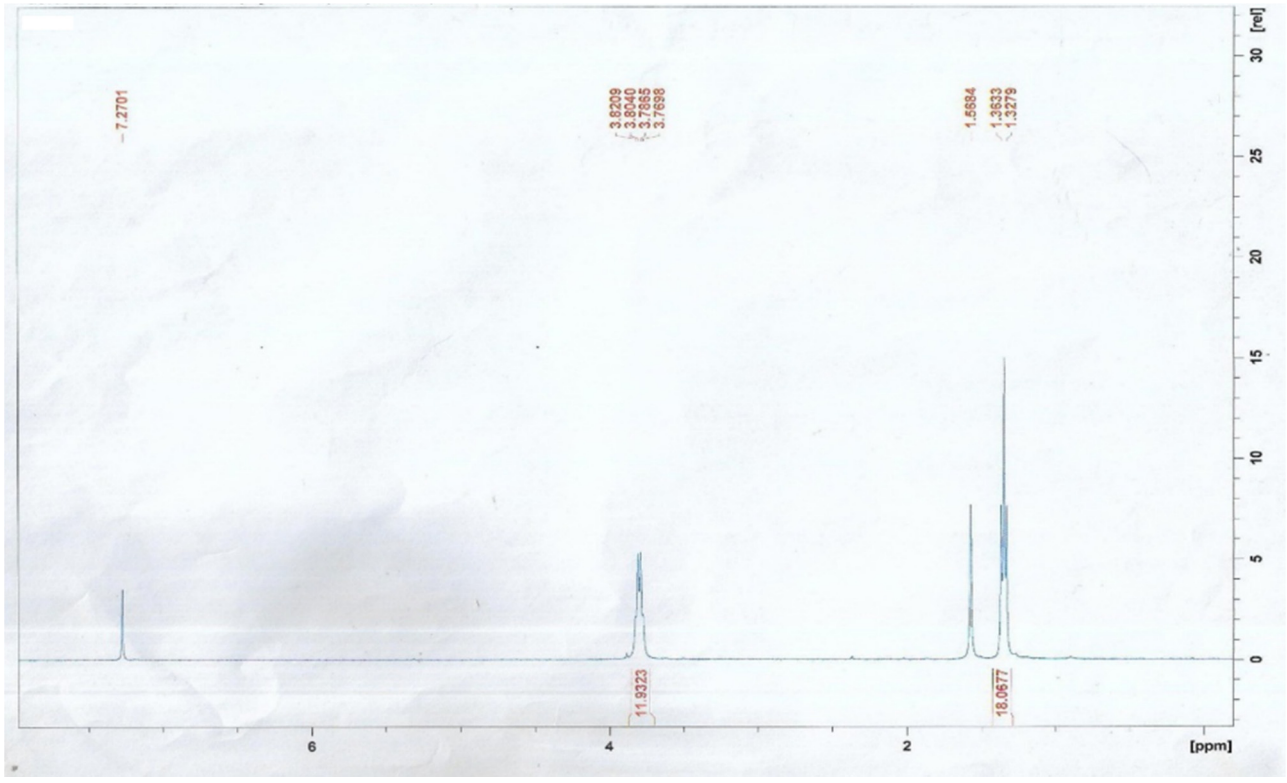

Figure A2: ^{1}H NMR spectrum of complex **1**.

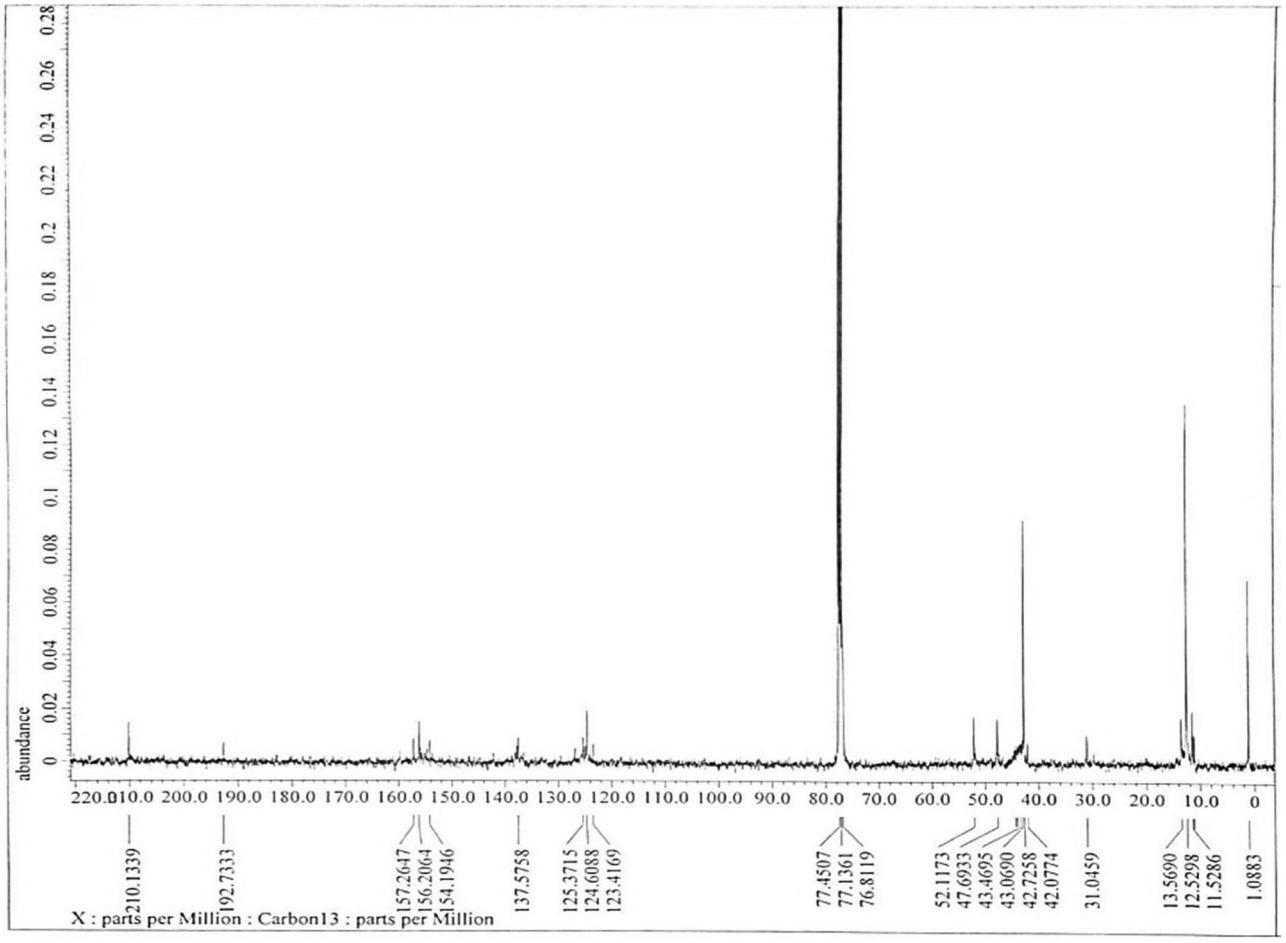

Figure A3: ^{13}C NMR spectrum of complex **1**.

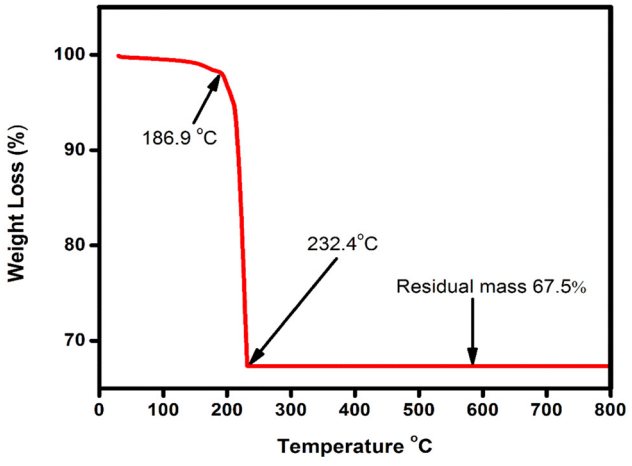

Figure A4: Thermogram of complex **1** showing weight loss as a function of temperature.

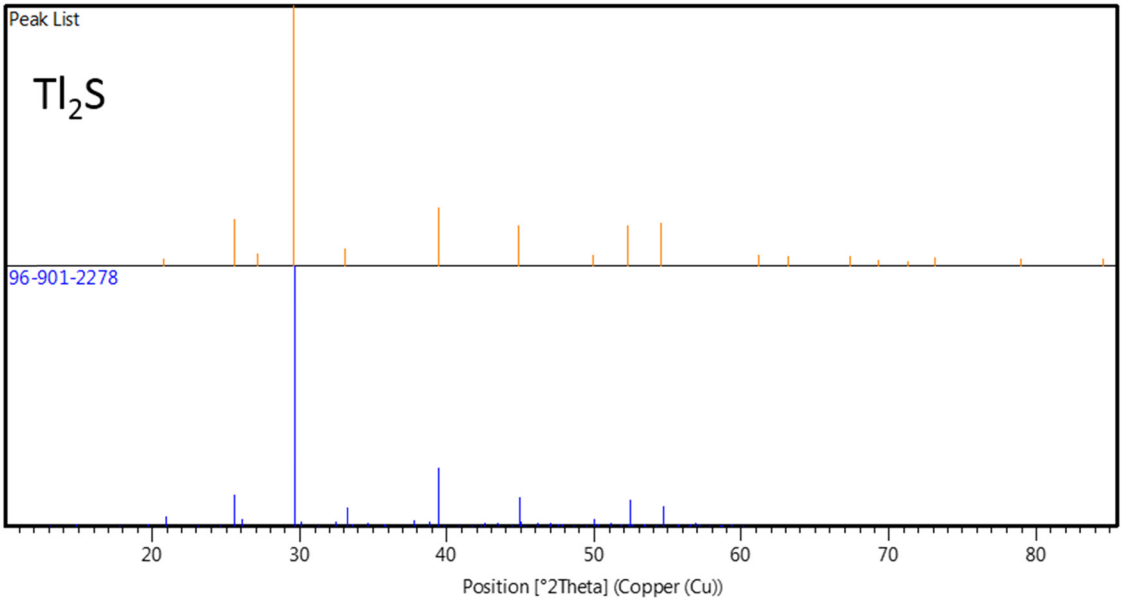

Figure A5: Standard pattern matching of Tl_2S thin films obtained by software available in X'Pert Highscore Diffractometer.

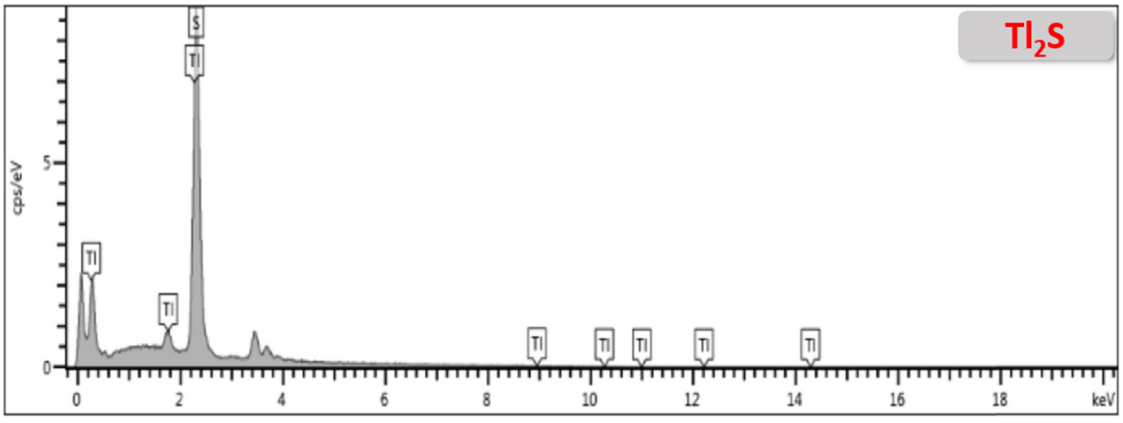

Figure A6: EDX spectra of Tl_2S thin films fabricated at 600°C confirms the presence of Tl and S.